Proceedings of the ASME Internal Combustion Engine Division 2010 Fall Conference
ICEF2010
September 12-15, 2010, San Antonio, Texas, USA

ICEF2010-35087

COMPARISON OF CRANKANGLE BASED IGNITION TIMING METHODS ON AN HCCI ENGINE

Ahmad Ghazimirsaied
Department of Mechanical Engineering
University of Alberta
Edmonton, Alberta T6G 2G8
Email: ghazimir@ualberta.ca

Mahdi Shahbakhti[1]
Charles Robert Koch[2*]
[1]Department of Mechanical Engineering
KNT University of Technology
Tehran, Iran
[2]Department of Mechanical Engineering
University of Alberta
Edmonton, AB T6G 2G8
Email: bob.koch@ualberta.ca

ABSTRACT

Autoignition timing of a mixture in Homogeneous Charge Compression Ignition (HCCI) is very dependant and sensitive to the engine operating condition. To characterize combustion timing, different crank angle dependant methods are used but these methods can exhibit inaccurate results at some operating conditions. In this paper, a criterion that divides the engine operating condition into two regions, low and high cyclic variations (unstable operation) is defined. Then, different crankangle based methods for determining the start of combustion inside the cylinder for each of the two regions are compared. The start and duration of combustion are compared for wide range of operating conditions and the relative merits of each method discussed. The methods for characterizing the start of combustion are: CA50 based on the total heat release; the start of combustion from the third derivative of the pressure trace with respect to crank angle; the start of combustion from the third derivative of the pressure trace with respect to crank angle with two limits; CA10 based on total heat release; CA10 based on peak of main stage of combustion. The last method is introduced in this paper and has advantages in terms of accuracy of ignition timing detection and correlation with the start of combustion particularly for high cyclic variation engine operation. A new criterion, defined as the ratio between peak of main stage and the sum of peak of main stage and cool flame stage of heat release, is introduced to more accurately identify the operating region of the engine. This criterion is used to understand the performance of each of those crank angle based methods. The performance of each of those methods is investigated for both the low cyclic variation and the high cyclic variation (unstable) region of the engine.

NOMENCLATURE

Ⓐ	Point A - Normal operating point
aBDC	after Bottom Dead Center
Ⓑ	Point B - Partial burn operating point
CAS	Combustion Analysis System
CA50	Crank Angle for 50% burnt fuel
CI	Compression Ignition
COV	Coefficient of Variation
ECU	Engine Control Unit
EGR	Exhaust Gas Recirculation
EVO	Exhaust Valve Opening
HCCI	Homogeneous Charge Compression Ignition
HTR_{max}	High Temperature Region Maximum Heat Release
HRR	total of peak of main stage and cool flame stage of heat release rate curve
IMEP	Indicated Mean Effective Pressure
IVC	Intake Valve Closing

*Address all correspondence to this author.

LTR_{max}	Low Temperature Region Maximum Heat Release
ON	Octane Number
Pman	Intake Manifold Pressure
Q_{HR}	Net Heat Release
PRF	Primary Reference Fuels
VVT	Variable Valve Timing
R_{HLTR}	$\frac{HTR_{max}}{HTR_{max}+LTR_{max}}$
RPM	Revolution Per Minute
SI	Spark Ignition
SOC	Start of Combustion
TDC	Top Dead Center
Tman	Intake Manifold Temperature
σ_{SOC}	Standard Deviation of Start of Combustion

1 INTRODUCTION

HCCI is considered as a high-efficiency alternative to spark-ignited (SI) gasoline operation and as a low-emissions alternative to traditional diesel compression ignition (CI) combustion. HCCI combustion has the potential for improved fuel economy, very low oxides of nitrogen (NOx) and low particulate emissions [1]. However, the practical application of HCCI requires overcoming several technical hurdles. HCCI misfire or partial-burn is undesirable because it results in increased exhaust emissions and reduces engine power output [2] but it is desirable to run the engine near this limit to maximize the high efficiency HCCI operating range.

At a fixed fuel octane and engine speed, HCCI operation is limited by partial burn at low load, and knock at high load - both undesirable phenomena [3]. Combustion-phasing retard [4, 5] is used to reduce HCCI engine knock at high loads. In this case, autoignition occurs during the expansion stroke where thermal stratification produced by heat transfer prolongs the duration of the staged autoignition lowering the peak heat-release rate [5,6,7]. This can help to reduce knock but to moderate excessive pressure rise rate, precise control of the combustion phasing is often required [2]. Beyond a particular combustion phasing, if the combustion is retarded too much, combustion becomes unstable [8] leading in partial-burn or misfire cycles. These factors restrict the extent of combustion-phasing retard but the exact behavior of the combustion for these conditions are not well known [9].

Increasing dilution rates eventually leads to misfire. Results show that both the start of combustion and burn duration are sensitive to mixture dilution (excess air or EGR). However, only the start of combustion is affected by the fuel octane number [10]. As fuel flow-rate is decreased, the net heat release rate decreases resulting in a decrease in the average combustion temperature which results in more unburned products characterized by high CO and unburned HC emissions and by increased cycle-to-cycle variations [3]. Results also show that the position of SOC (Start of Combustion) plays an important role in cyclic variations of HCCI combustion with less variation observed when SOC occurs immediately after top dead centre (TDC) [11]. Higher levels of cyclic variations are observed in the main (second) stage of HCCI combustion compared with that of the first stage for the Primary Reference Fuel (PRF) fuels studied. Cyclic variation of SOC is a function of charge properties and increases with an increase in the EGR rate, but decreases with an increase in equivalence ratio, intake temperature, and coolant temperature [11].

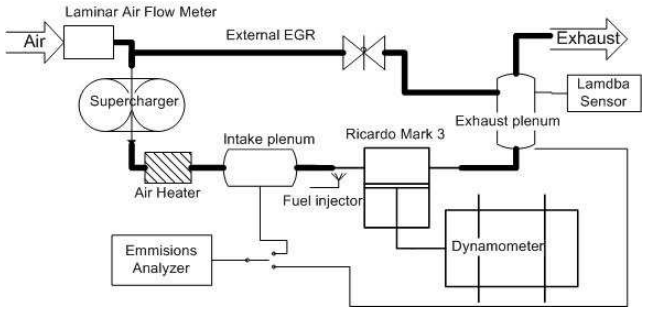

FIGURE 1. Schematic of the experimental setup.

The combustion phasing is a critical factor in HCCI combustion since it affects the power, fuel combustion and exhaust emissions [12]. The combustion phasing could be defined as when the start of combustion *(SOC)* occurs [13]. Main factors that effect the start of combustion for HCCI are investigated in [14]. In [15], the effect of employing different SOC methods on the low temperature combustion (LTC) phase is investigated.

The goal of this study is to find an accurate measurement method for HCCI combustion timing that works for both normal and partial burn operating conditions. The remainder of this paper is as follows: the single cylinder experimental setup is described; a criterion for determining a partial burn cycle is defined; SOC is characterized using existing methods and a new method is introduced that shows better SOC determination for engine operation with high cyclic variation; finally, the analysis is extended to all operating points in order to check the performance of the methods over a wide range of operating conditions.

2 ENGINE SETUP

A single cylinder Ricardo Hydra Mark 3 block fitted with a VVT Mercedes E550 cylinder head [16] is shown schematically in Figure 1 with specifications given in Table 1 [17]. This spark ignition engine is outfitted with a Kistler piezo-electric pressure transducer. The intake air is heated with a temperature controlled 600W electric heater, while the intake pressure is adjusted with an externally driven supercharger. Primary Reference Fuels (N-heptane and iso-octane) are individually port injected to set octane values with two injectors driven by a dSpace-MicroAutobox ECU.

TABLE 1. Configuration of the Ricardo single-cylinder engine

Parameters	Values
Bore $\times$ stroke [mm]	97×88.9
Compression Ratio	12
Displacement [L]	0.653
Connecting Rod Length [mm]	159
Valves	4
Valve Lift [mm]	9.3

TABLE 2. Engine operating conditions

Parameter	Range
Manifold Pressure [*kPa*]	90-120
Manifold Temperature [$^\circ$C]	85-97
External EGR [%]	0
Fuel Octane Number [PRF]	0,10,20,30,40
Engine Speed [RPM]	1021-1074
Equivalence Ratio [-]	0.29-0.55

Cylinder pressure is recorded 3600 times per crank revolution, and then analyzed for the pertinent combustion metrics, such as IMEP (Indicated Mean Effective Pressure), ignition timing and burn duration. All other parameters are logged at 100 Hz using A&D Baseline DAC. Engine operating points spanning the range from normal operation to misfire at fixed engine RPM but varying other inputs are summarized in Table 2. All of the 115 engine operating points are at steady-state operating conditions (inputs to engine and engine speed held constant) and 300 engine cycles of cylinder pressure data are recorded for each.

Fuels like paraffin which have a two stage heat release are considered in this paper. We consider only octane numbers from 0 to 40 since our engine will only operate smoothly in this range. Above an octane of 40, the ignition delay is too long and unstable operation results.
NOx emissions and indicated specific fuel consumption increase as the octane number is increased due to lower dilution and higher peak temperatures [10]. Yao et al. found that their HCCI engine did not run smoothly at high octane numbers. In addition, HCCI combustion efficiency increases with the decrease of the octane number and HC emissions increase with the increase of octane number because of the retarded ignition timing and decreased combustion temperature [18]. Thus our operating range reflects the desired HCCI operation while considering the limitations of our engine.

3 Background

To develop robust ignition timing methods during partial burn and misfire it is essential to be able to identify partial burns. The coefficient of variation of IMEP, *COVImep*, is a measure of cyclic variability of engine parameters [11]. To identify a partial burn with IMEP several criteria have been developed [3, 9, 17]. For example, a standard deviation of IMEP greater than 2%, indicates the appearance of partial burn and misfire cycles [9]. Applying this criterion to our 115 engine operating points, it is found that *COVImep* is not a reliable parameter in recognizing high cyclic variation. For example several operating points having high *COVImep* but have few or zero partial burn cycles.

A partial burn cycle is defined as when the total heat release is less than 90% of previous cycle. That is, a cycle with 10% reduction in total heat release compared to its previous cycle is considered as a partial burn cycle [9]. An experimental operating point is considered as an partial burn operating point if it contains more than 14% partial burn cycles [2].

4 SOC Results - Two Experimental Points

To compare and understand existing SOC methods and the new SOC method, two representative operating points from the 115 operating points have been selected. These points represent low (Point Ⓐ) and high (Point Ⓑ) cyclic variations (partial burn region). Consecutive cycle total heat release for these two operating points for the 300 engine cycles are shown in Figure 2 and Figure 3. The number of partial burn cycles are 0% for Ⓐ in Figure 2 and 33% for Ⓑ in Figure 3 respectively. In these figures the number of cycles with reduction in total heat release is higher in Ⓑ compared to the Ⓐ resulting in considerable reduction in total heat release in Ⓑ. In the next section, different ignition timing methods applied are evaluated for these two cases. Then, methods that work well for these two operating points are evaluated at all 115 operating points.

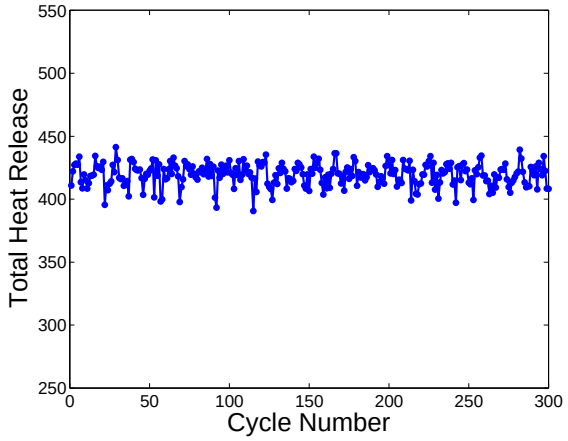

FIGURE 2. Ⓐ - Normal Conditions, low cyclic variations: speed 1025 RPM, Trunner 81 °C, Pman 115 kPa, ON 30, λ 2.28, Total HR 420 j, COVImep 1.7percent, Percentage of partial burn cycles 0

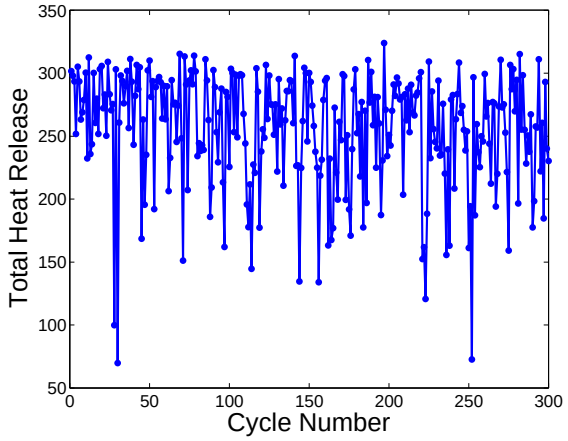

FIGURE 3. Ⓑ - Partial Burn Conditions, high cyclic variations: speed 1025 RPM, Trunner 80 °C, Pman 95 kPa, ON 0, λ 2.61, Total HR 232 j, COVImep 28percent, Percentage of partial burn cycles 33.18

4.1 CA50

This method characterizes ignition timing using CA50 (the crank angle of 50 % Q_{HR}) [13, 19, 20, 21]. It will be shown later that CA50 combines both the location and duration of combustion making it unsuitable as a single measure of ignition timing. With this method, the calculation of CA50 can only occur after the expansion stroke is finished leading to a delay which could be a disadvantage in cycle-to-cycle control applications [20]. The detection of CA50 on the main stage of combustion is regarded as the correct detected SOC for the CA50 method.

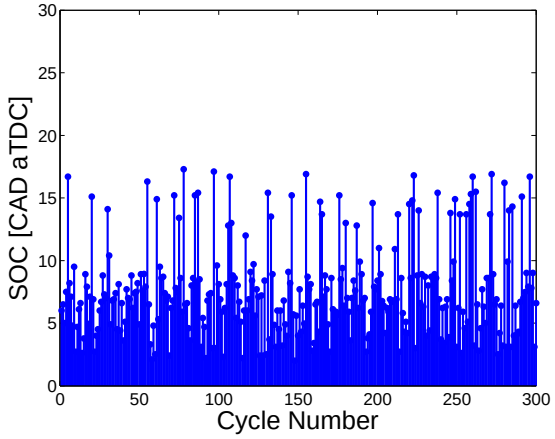

FIGURE 4. Cyclic variation trend of SOC for Ⓐ with Normal Conditions: Same conditions as in Figure 2

4.2 Pressure 3rd derivative

In the crank angle region near TDC during compression, the pressure trace history has a negative concavity, which becomes positive during ignition (i.e. a positive third derivative). This transition from negative to positive concavity is considered as the point of ignition [22, 23]. SOC is defined as being the point at which the third derivative of the pressure trace with respect to the crank angle, θ, exceeds a heuristically determined limit:

$$\frac{d^3P}{d\theta^3} > \frac{d^3P}{d\theta^3}\,|_{lim} = 0.030[\frac{kPa}{CAD^3}] \qquad (1)$$

The limit is selected such that the point of ignition represents the change in concavity but is not affected by noise in the differential signal.

Applying this method to the normal operating point Ⓐ SOC for all 300 cycles is shown in Figure 4. This is typical behavior of SOC cyclic variation in most of the operating points without too many partial burn cycles. However, if partial burn cycles appear in the operating point, this criterion does not work since the transition from negative to positive concavity does not exist clearly anymore. This is shown in Figure 5 for Ⓑ where many cycles have weak combustion resulting in undetected SOC. This method correctly identifies 100% SOC of Ⓐ and 8.7% SOC of Ⓑ. Hence this method for determining SOC does not perform well for operating points with partial burn cycles. Having no point (based on 2 rev crankangle data) above the determined limit of Equation 1 or having several points above the above-mentioned limit with the same magnitude is considered as the incorrectly detected SOC. To illustrate this concept more discussions can be found in the Appendix.

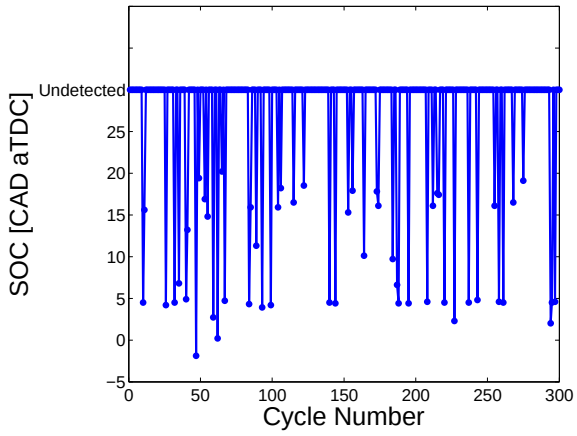

FIGURE 5. Cyclic variation trend of SOC for Ⓑ with Partial Burn Conditions: Same conditions as in Figure 3

4.3 Pressure 3rd derivative - 2 limits

In order to improve the performance of Pressure 3rd derivative method, two limits in Equation 1 are determined for different loads of the engine. For operating points with an average IMEP of less than 2.91 the third derivative of the pressure trace with respect to the crank angle θ should exceed a heuristically determined limit 0.020 and for the ones with average IMEP higher than 2.91 the limit would be 0.030. Although these new limits increase the percentage of correct detected SOC the lack of concavity for operating points with high number of partial burn cycles still remains. This method correctly identifies 99% SOC of Ⓐ and 50% SOC of Ⓑ. In the case of having no point above the two determined limits for this method or having several points above the above-mentioned limits with the same magnitude, the detected angle is considered as incorrectly detected SOC.

4.4 CA10 - total

CA10 is a parameter used in literature as start of combustion indicator. It is defined as the crank angle where 10 percent of total heat release of combustion has occurred. This criterion is widely [15] used but can fail (see next method) for fuels with a low temperature reaction (LTR) and a subsequent poor main stage high temperature reaction (HTR). This method correctly identifies 100% SOC of Ⓐ but only 53% SOC of Ⓑ. The detection of CA10 on the main stage of combustion is regarded as the correctly detected SOC for the CA10 method.

4.5 CA10 - main stage

CA10-main is a new method defined as 10 percent of the maximum heat release of only the main stage. This method does not have the disadvantages of CA10-total since it does not jump back to cool flame stage of combustion for same operating conditions.

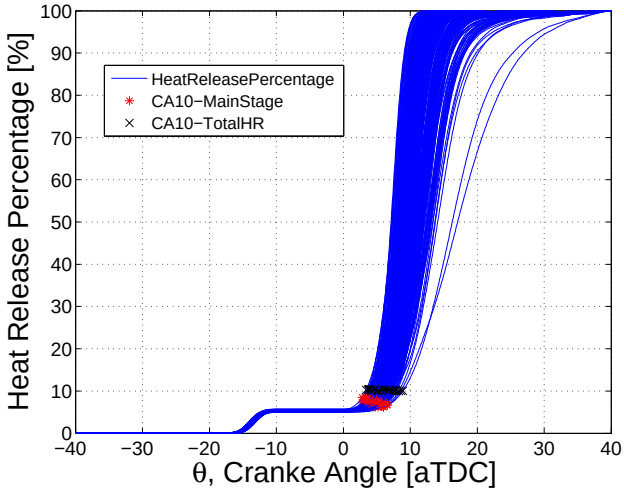

FIGURE 6. Heat Release Ⓐ with Normal Conditions: Same conditions as in Figure 2, CA10PercentageMainStage 100

The heat release percentage as a function of crank angle with their calculated CA10-total and CA10-main are shown in Figure 6 and Figure 7 for Ⓐ and Ⓑ respectively. All of the calculated CA10-total are on the main stage of combustion for Ⓐ (normal condition) in Figure 6. However, for Ⓑ (partial burn case) as shown in Figure 7, 47 percent of cycles have CA10-total at the low temperature region of combustion, which gives an erroneous SOC. However, the CA10-main method correctly identifies 100% SOC of Ⓐ and 100% SOC of Ⓑ since it does not jump to the low temperature region. The detection of CA10 on the main stage of combustion is regarded as the correctly detected SOC for the CA10 methods.

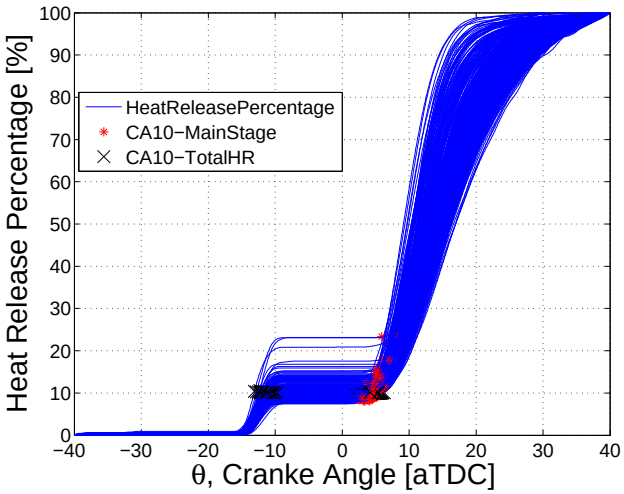

FIGURE 7. Heat Release Ⓑ with Partial Burn Conditions: Same conditions as in Figure 3, CA10PercentageMainStage 100

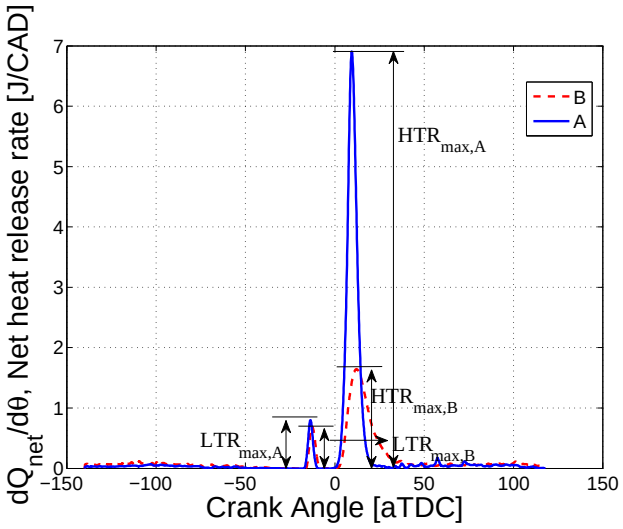

FIGURE 8. Heat release rate and HTR TO LTR peak definition for two sample points Ⓐ and Ⓑ

A new criterion, called $HTR\ to\ HTR+LTR$ ratio, is defined to quantify the improved performance of CA10-main method compared to CA10-total. This is defined as $R_{HLTR} = \frac{HTR_{max}}{HTR_{max}+LTR_{max}}$ the ratio of peak of main stage to total of peak of main stage and cool flame stage of heat release rate curve. R_{HLTR} can be used as a real-time criterion to detect the partial burn region for cycle-to-cycle control purposes. For two points Ⓐ and Ⓑ R_{HLTR} is 0.91 and 0.69 espectively as shown in Figure 8.

The relation between R_{HLTR} and the location of CA10 for Ⓑ, is shown in Figure 9. This figure reflects the effect of R_{HLTR}

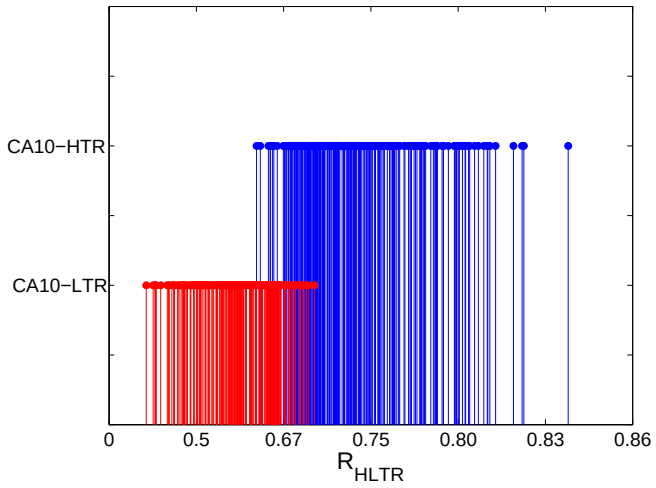

FIGURE 9. Effect of $HTR\ to\ HTR+LTR$ peak ratio on location of CA10 for Ⓑ

on the location of CA10. There is a clear boundary between CA10 on main stage and cool flame stage of combustion according to the specific R_{HLTR} of the corresponding cycle. The taller (blue) bars correspond to the R_{HLTR} where CA10 occur on the main stage while the shorter (red) bars correspond to the cool flame stage of combustion. Figure 9 shows that for $R_{HLTR} > 0.73$, CA10 always occur on the main stage of combustion.

4.6 Summary for Ⓐ and Ⓑ

Table 3 summarizes the performance of the five methods applied to Ⓐ and Ⓑ showing what percentage of cycles SOC was correctly identified. This paper focuses on steady-state operating points. The smaller the deviation of SOC would be, the more consistent the ignition timing detection will be for a steady state operating point with no change in operating conditions. Therefore, the smaller the standard deviation of the SOC is, the more robust the method will be.

TABLE 3. Summary of standard deviation of SOC (σ_{SOC}) and percent of correctly detected SOC for methods: ① CA50, ② Pressure 3rd derivative, ③ Pressure 3rd derivative with two limits, ④ CA10-total and ⑤ CA10-main for operating points Ⓐ and Ⓑ (0 and 33% partial burn cycles)

Methods	SOC (Deg)		σ_{SOC} (Deg)		$SOC_{Correct-det}$	
-	Ⓐ	Ⓑ	Ⓐ	Ⓑ	Ⓐ	Ⓑ
①	10	14	1.59	1.6	100	100
②	8.4	28.3	5.4	5.8	100	8.7
③	5.5	17.3	4.4	13.5	98.7	49.6
④	5.7	-1.9	0.98	7.8	100	53
⑤	4.6	13.4	0.78	0.83	100	100

Table 4 rates the performance of all the methods for both Ⓐ (normal) and Ⓑ (partial burn) operating conditions based on the requirement to correctly detect SOC for all cycles. The only two methods which satisfy this for both Ⓐ and Ⓑ are CA50 and CA10-main. Since CA50 combines combustion duration and SOC, CA10-main is the best method for determining SOC for these two cases. Validating these results on all 115 operating conditions is contained in the next section.

TABLE 4. Method rating for Ⓐ and Ⓑ - ($\surd$ -acceptable, $\times$ -not acceptable)

Methods	Ⓐ	Ⓑ
CA50	$\surd$	$\surd$
Pressure 3rd derivative	$\surd$	$\times$
Pressure 3rd derivative - two limits	$\surd$	$\times$
CA10-total	$\surd$	$\times$
CA10-main	$\surd$	$\surd$

5 Results for all operating points

Lambda versus the IMEP, for all 115 operating points is shown in Figure 10 to provide an overview of the conditions tested.

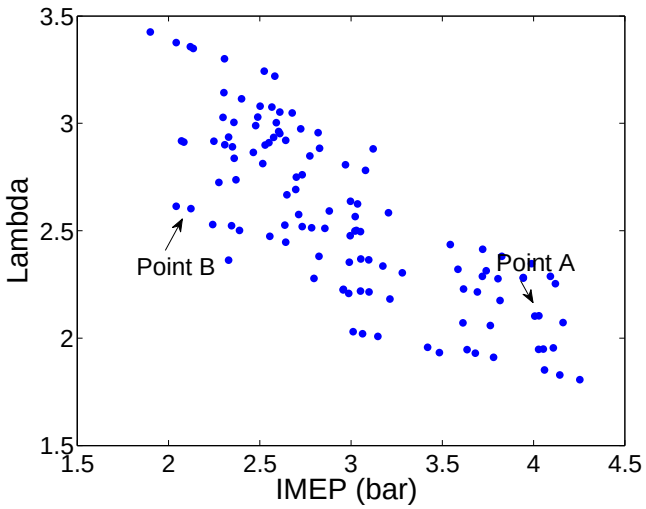

FIGURE 10. Lambda versus engine load

5.1 Discussion of SOC Methods

CA50 Method

Figure 11 shows that there is no strong correlation between CA50 and burn duration (CA10-CA90) for 115 operating points.

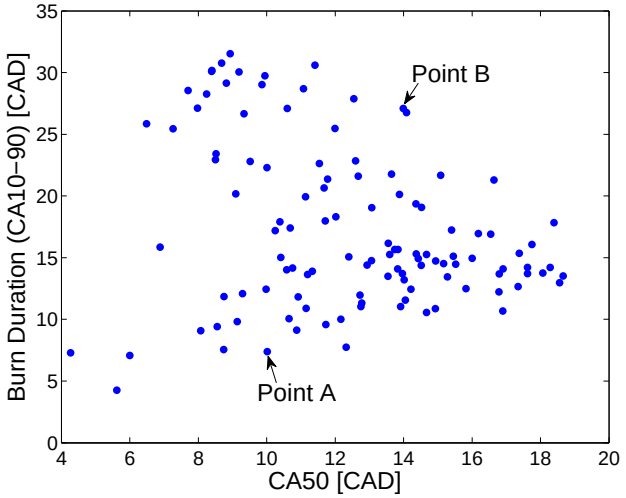

FIGURE 11. Mean of burn duration versus CA50

This is further illustrated in Figure 12 which shows how mean (of 300 cycles) of CA50 change as a function of the mean of SOC (determined from 3rd derivative of pressure). Two different regions can be distinguished in Figure 12. An almost linear correlation with deviations from linear trend between mean

of CA50 as a function of SOC is observed in region-I so CA50 could be approximately determined from SOC but not vice versa. In region-II, no trend can be observed between CA50 and SOC implying that CA50 does not necessarily provide a good measure of SOC. Only the percentage of correctly detected SOC cycles in each operating point excluding the cycles with incorrect or undetected SOC, is shown in Figure 12 with the average value of correctly determined SOC cycles shown on the x-axis.

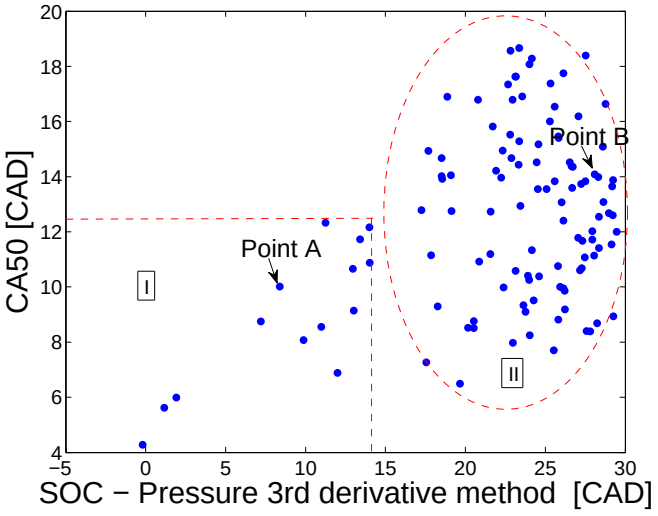

FIGURE 12. Mean of CA50 versus mean of SOC (Pressure 3rd derivative)

Third derivative method

The performance of the pressure 3rd derivative method when it is applied to all operating points by plotting the percentage of correct detected SOC (Not weak or misfire) versus percentage of partial burn cycles is shown in Figure 13. The figure shows that as the percentage of partial burn cycles increases the percentage of correct detected SOC decreases. Thus confirming that the 3rd derivative method is not an accurate method for all operating points.

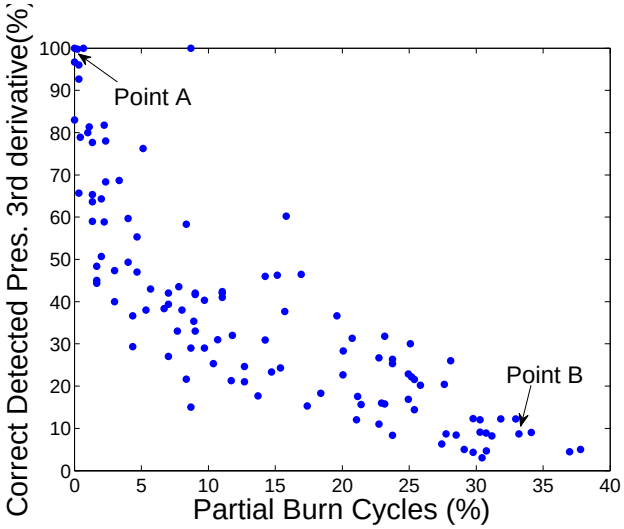

FIGURE 13. Percentage of correct detected SOC versus percentage of partial burn cycles

5.2 Comparison on crank angle based parameters

To compare the performance of the four crank angle based methods covered in this paper, the percentage of correctly detected cycles of ignition timing versus cumulative percentage of all 115 operating points is shown in Figure 14, The cumulative percentage of all operating points is plotted on the x-axis versus the maximum or lower number of correctly detected ignition timing cycles on the y-axis. For example, considering the SOC (red solid) curve, 13% of the operating points have their SOC event correctly determined for 30 cycles or less out of 300. The slope of the curve is relatively low indicating the slow growth of percentage of cycles with correctly detected ignition timing. Thus the pressure 3rd derivative curve is the worst performer when compared to the other methods. The method CA10-main has the best performance (green dot-dashed curve) with a high slope meaning that for almost all the operating points SOC is correctly determined for all 300 out of 300 cycles.

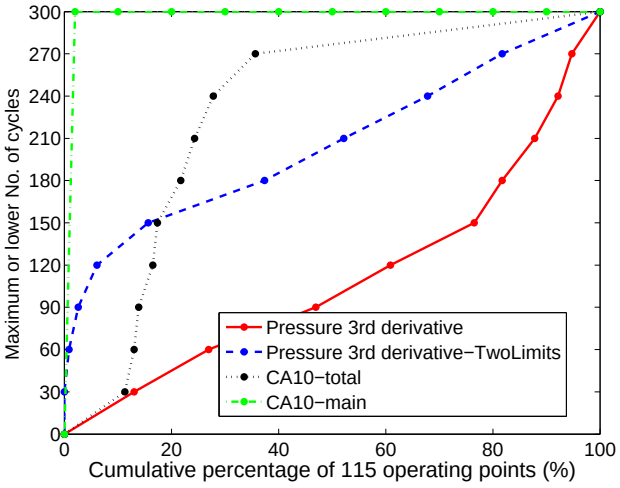

FIGURE 14. Cumulative percentage of operating points versus maximum or lower number of cycles where ignition timing is correctly identified for four different SOC methods based on the pressure 3rd derivative, pressure 3rd derivative - two limits, CA10-total and CA10-main

For each of the 115 operating points SOC is calculated for the 300 cycles (eliminating weak or misfire cycles) and the standard deviation is then calculated. The highest and lowest values of standard deviation for all 115 points is found for four methods and is listed in Table 5. The maximum and minimum standard deviation of SOC decreases down the table. The maximum standard deviation of CA10-main is the smallest (1.1 CAD) showing that with this criterion the variation of the location of ignition timing does not vary much at each of the 115 operating points and as such it seems to be the most robust method of determining SOC. Standard deviation of calculated CA10 based on main stage for all the operating points are shown in Figure 15.

TABLE 5. Standard deviation of SOC for all 115 points

Method	Min (deg)	Max (deg)
Pressure 3rd derivative	1.6	13.5
Pressure 3rd derivative-two limits	1.3	12.0
CA10-total	0.2	7.8
CA10-main	0.5	1.1

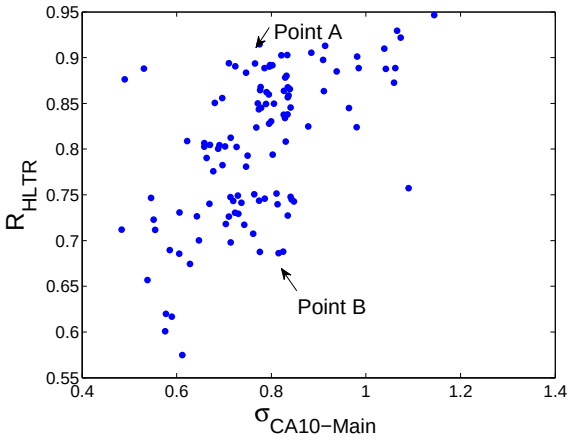

FIGURE 15. R_{HLTR} versus Standard deviation of CA10-main

In Figure 16, R_{HLTR} versus Partial Burn Cycles percentage is shown for all 115 operating points with different symbols for different octane numbers. A general trend in Figure 16 is that a higher percentage of partial burn cycles in the operating point and hence higher cyclic variations corresponds to a lower R_{HLTR}. Also R_{HLTR} is observed to be generally lower for fuels with lower octane number.

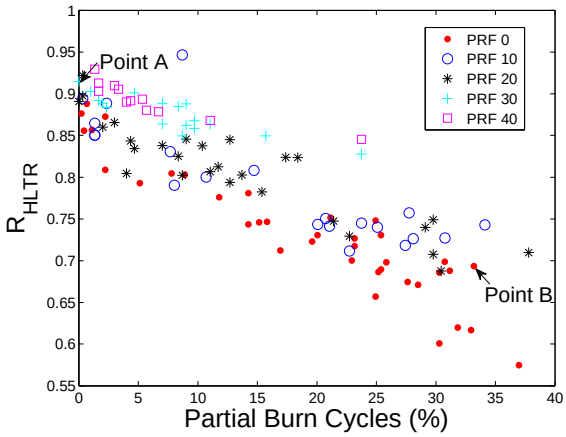

FIGURE 16. R_{HLTR} versus partial burn cycles for all the data points

Conclusions

A partial burn cycle of the engine is identified when the heat release is 90% of the previous cycle. The criterion for characterizing an HCCI engine operation point as partial burn is when 14% of the 300 cycles are partial burn cycles. Based on this criterion, two operating points in the normal and partial burn region of the engine are examined and the performance of five methods for characterizing the combustion timing are investigated and compared. Examining combustion criterion it is found that the four existing methods are not effective during partial burn operation but a new criterion CA10 based on the main stage of combustion is effective. The results for 115 operating points over a wide range of operating conditions at a fixed engine speed demonstrate that this new criterion is the most effective measure of combustion timing.

Future Work

The new method could be useful in extending the engine operation region using control of ignition timing in our HCCI engine near the partial burn and misfire operating condition [19].

ACKNOWLEDGMENT

AUTO21 Network of Centres of Excellence, the Canadian Foundation for Innovation (CFI) and the Natural Sciences and Engineering Research Council of Canada (NSERC) are gratefully acknowledged.

REFERENCES

[1] Stanglmaier, R., and Roberts, C., 1999. "Homogeneous charge compression ignition (HCCI): Benefits, compromises, and future engine applications". *SAE Paper No. 1999-01-3682.*, ***108***.

[2] Ghazimirsaied, S., Shahbakhti, M., and Koch, C. R., May 11-13, 2009. "Partial-burn crankangle limit criteria comparison on an experimental HCCI engine". *Proceeding of Combustion Institue - Canadian Section Spring Technical Meeting, University of Montreal, Quebec.*

[3] Zhao, H., 2007. *HCCI and CAI engines for the automotive industry*. Woodhead Publishing Limited.

[4] Sjoberg, M., Dec, J., Babajimopoulos, A., and Assanis, D., 2004. "Comparing enhanced natural thermal stratification against retarded combustion phasing for smoothing of HCCI heat-release rates". *SAE Paper No. 2004-01-2994.*

[5] Sjoberg, M., Dec, J. E., and Cernansky, N. P., 2005. "Potential of thermal stratification and combustion retard for reducing pressure-rise rates in HCCI engines, based on multi-zone modelling and experiments". *SAE Paper No. 2005-01-0113.*

[6] Dec, J. E., Hwang, W., and Sjoberg, M., 2006. "An investigation of thermal stratification in HCCI engines using chemiluminescence imaging". *SAE Paper No. 2006-01-1518.*

[7] Olsson, J.-O., Tunestal, P., Johansson, B., Fiveland, S., Agama, J., and Assanis, D., 2002. "Compression ratio influence on maximum load of a natural gas- fueled HCCI engine". *SAE Paper No. 2002-01-0111.*

[8] Olsson, J.-O., Erlandsson, O., and Johansson, B., 2000. "Experiments and simulation of a six-cylinder HCCI engine". *SAE Paper No. 2000-01-2867.*

[9] Sjoberg, M., and Dec, J. E., 2007. "Comparing late-cycle autoignition stability for single- and two-stage ignition fuels in HCCI engines". *Proceeding of Combustion Institue,* ***31***, pp. 2895–2902.

[10] Atkins, M. J., and Koch, C. R., 2005. "The effect of fuel octane and diluent on HCCI combustion". *Proceeding of the Institution of Mechanical Engineering, Part D: Journal of Automobile Engineering,* ***219***, pp. 665 – 675.

[11] Shahbakhti, M., and Koch, C. R., 2008. "Characterizing the cyclic variability of ignition timing in a HCCI engine fueled with n-heptane/iso-octane blend fuels". *International Journal of Engine Research,* ***9***, pp. 361 – 397.

[12] Choe, D., Lee, M., Lee, K., and Sunwoo, M., 2007. "SOC detection of controlled auto-ignition engine". *SAE Paper No. 2007-01-3538.*

[13] Bengtsson, J., 2004. "Closed-loop control of HCCI engine dynamics". PhD thesis, Lund Institute of Technology,.

[14] Chiang, C. J., and Stefanopoulou, A. G., 2006. "Sensitivity analysis of combustion timing and duration of HCCI engines". *Proceeding of the 2006 American Control Conference, Minneapolis, USA.*

[15] Northrop, W. F., Bohac, S. V., and Assanis, D. N., 2009. "Premixed low temperature combustion of biodiesel and

blends in high speed compression ignition engine". *SAE Paper No. 2009-01-0133*.
[16] Lupul, R., 2008. "Steady state and transient characterization of a HCCI engine with varying octane fuel". Master's thesis, University of Alberta.
[17] Audet, A., 2008. "Closed loop control of HCCI using camshaft phasing and dual fuels". Master's thesis, University of Alberta.
[18] Yao, M., Zheng, Z., Zhang, B., and Chen, Z., 2004. "The Effect of PRF Fuel Octane Number on HCCI Operation". *SAE Paper No. 2004-01-2992*.
[19] Ghazimirsaied, A., Shahbakhti, M., and Koch, C. R., 2010. "HCCI engine combustion phasing prediction using a symbolic-statistics approach". *Journal of Engineering for Gas Turbines and Power, In Press*.
[20] Bengtsson, J., Strandh, P., Johansson, R., Tunestal, P., and Johansson, B., 2004. "Closed-loop combustion control of HCCI engine dynamics". *International Journal of Adaptive Control and Signal Processing,* ***18***, pp. 167–179.
[21] Ghazimirsaied, A., Shahbakhti, M., Audet, A., and Koch, C. R., 2008. "HCCI engine cyclic variation characterization using both chaotic and statistical approach". *Proceeding of Combustion Institue-Canadian Section, Spring Technical Meeting, University of Toronto, Ontario*.
[22] Checkel, M. D., and Dale, D. J., 1986. "Computerized knock detection from engine pressure records". *SAE Paper No. 860028*.
[23] Kirchen, P., Shahbakhti, M., and Koch, C. R., 2007. "A skeletal kinetic mechanism for PRF combustion in HCCI engines". *Combustion Science and Technology,* ***179***, pp. 1059–1083.

APPENDIX: ERRONEOUS PRESSURE 3RD DERIVATIVE DETECTION

To illustrate this, the third derivative of pressure along with the pressure trace is shown in Figure 17 for a cycle of normal sample point Ⓐ and is shown in Figure 18 for a cycle of partial burn sample point Ⓑ.

As it can be seen in Figure 18, the choice of an acceptable heuristically determined limit for point Ⓐ is not able to detect any sharp rise in point Ⓑ. This undetected SOC is considered as an erroneous SOC prediction.

Changing the choice of heuristically determined limit for another cycle of same sample partial burn point Ⓑ is shown in Figure 19. Although there are many points detected above the limit, there is still no single clear spike in the 3rd derivative of mean pressure regardless of the value of the limit. This is another example of erroneous SOC detection.

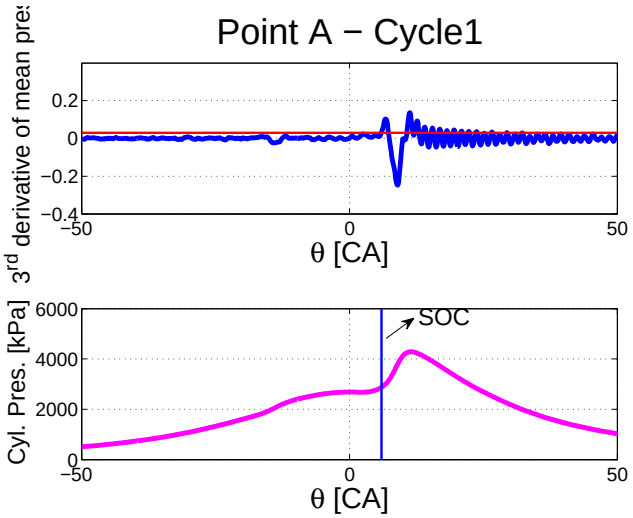

FIGURE 17. third derivative of pressure with its pressure trace

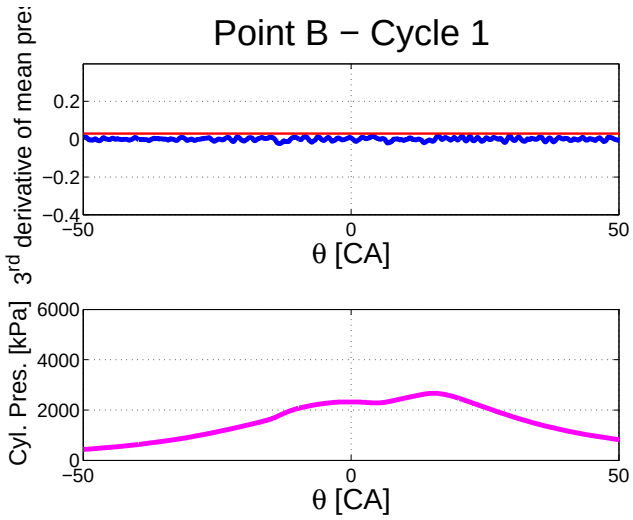

FIGURE 18. third derivative of pressure with its pressure trace for a partial burn point B for a cycle with undetected SOC

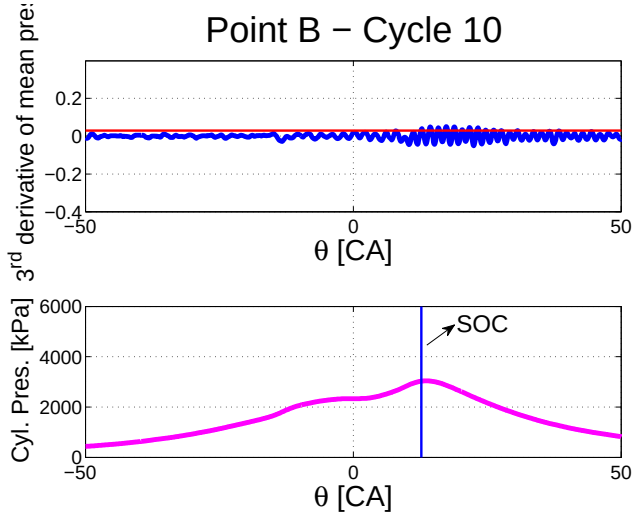

FIGURE 19. third derivative of pressure with its pressure trace for a partial burn point B for a cycle with detected SOC but no sharp rise from limit